RSC Advances

PAPER

View Article Online
View Journal | View Issue

Cite this: *RSC Adv.*, 2021, **11**, 2083

Rapid and continuous fabrication of TiO_2 nanoparticles encapsulated by polyimide fine particles using a multistep flow-system and their application†

Takayuki Ishizaka, *[a] Maya Chatterjee [a] and Hajime Kawanami *[b]

Received 19th November 2020
Accepted 17th December 2020

DOI: 10.1039/d0ra09810h

rsc.li/rsc-advances

PI fine particles encapsulating a large number of TiO_2 nanoparticles (PI FPs/TiO_2 NPs) were successfully fabricated rapidly and continuously by the emulsion re-precipitation method using a multistep flow synthetic system. The fabricated material, PI FPs/TiO_2 NPs, was spherical in structure with a diameter of 214 nm, and the mean size of TiO_2 NPs was 5.2 nm. Line scan elemental analysis with SEM-EDX showed that the TiO_2 NPs were disproportionately embedded near the surface of the PI FPs. UV-vis transmission spectra revealed high UV shielding efficiency of the PI FPs/TiO_2 NPs as the NPs are located near the surface.

1. Introduction

Nanotechnologies or nanomaterials have been used in a wide range of applications. Titanium dioxide nanoparticles (TiO_2 NPs) are one of the most promising nanomaterials because of their frequent applications in different fields such as catalysts, pharmaceuticals, paints, plastics, papers, inks, foods, toothpastes, cosmetic products as a UV-shielding material, and white pigments on the commercial, industrial, and environmental scale.[1–6] TiO_2 is a white pigment with excellent brightness and a very high refractive index, and up to 36% of the food-grade TiO_2 has been used in an ultrafine form as a white coloring agent in confectioneries, sauces, cakes, and pastries.[7] For example, over 40% of TiO_2 particles in commercial gums are TiO_2 NPs. However, the potential risk of TiO_2 NPs on human health has drawn attention that it can leach out and be swallowed when chewing in the case of gums, and the human dietary exposure dose of TiO_2 NPs has reached 2.16 to 100 microgram per kilogram body weight per day.[3,8–10]

The definition of nanomaterials generally refers to particles of 1–100 nm. Along with enormous studies on technological and economic potential, the risks of handling nanomaterials such as TiO_2 NPs have been reported. During handling, inhaled TiO_2 NPs are translocated to the brain and/or other organs like a kidney and a liver, which can cause carcinogenesis, genotoxicity, and immune disruption.[4] As for other possible exposure routes, there are a few reports on dermal penetration. In those reports, the toxicological properties of TiO_2 particles are mainly based on the particle size, which drastically decreased with the increasing size.[2,3,9] In addition, coarse and fine particles (FPs, >100 nm) are no longer toxic materials in humans and animals.[2] Therefore, for the use of TiO_2 NPs in consumer products, the size should be larger than 100 nm to avoid the potential risk with regard to human health. The development of NPs for use in cosmetics requires introduction of some specific properties to avoid health impairments and effective passage through the skin. In this paper, we report the development of the fabrication method by using a multistep microfluidic system and succeeded in encapsulating a large number of TiO_2 NPs in a polymer-based fine particle (>100 nm), which might be the effective way to develop a suitable material without any health impairments.

To obtain polymer-based FP encapsulating inorganic NPs, various methods such as self-assembly encapsulation,[11] layer-by-layer deposition,[12] cross-linking of polymeric micelles surrounding the inorganic cores,[13–15] emulsion polymerization including suspension polymerization, and mini emulsion polymerization[16–19] have been developed and employed to fabricate a polymer-based FP with a single inorganic NP core. Among these methods, the emulsion polymerization methods have provided a polymer-based FP encapsulating not only a single NP (particle size: 10 nm to sub-μm) but multiple NPs (particle size: 5 nm to 30 nm). Polystyrene and poly(methyl methacrylate) FPs with highly concentrated inorganic NPs were obtained by a two-step process, that is, preparation of mini emulsions containing inorganic NPs, followed by polymerization under heating for several hours.[17–19]

Previously, we demonstrated the continuous fabrication of polyimide (PI) FPs *via* re-precipitation using a multistep flow-

[a]*Research Institute for Chemical Process Technology, National Institute of Advanced Industrial Science and Technology (AIST), 4-2-1 Nigatake, Miyagino-ku, Sendai, Miyagi 983-8551, Japan. E-mail: t-ishizaka@aist.go.jp*

[b]*Interdisciplinary Research Center for Catalytic Chemistry, National Institute of Advanced Industrial Science and Technology (AIST), Central 5, 1-1-1 Higashi, Tsukuba, Ibaraki 305-8565, Japan. E-mail: h-kawanami@aist.go.jp*

† Electronic supplementary information (ESI) available. See DOI: 10.1039/d0ra09810h

system.[20,21] In this emulsion re-precipitation method, two-step operations, *i.e.*, preparation of droplets of polymer solution dispersed in *n*-hexane followed by the formation of polymer FPs *via* re-precipitation using thermal treatment, were sequentially and rapidly performed within very short times (*ca.* 10 s). Hence, when NPs are quasi-stably dispersed into polymer solution by mixing inside the system, they could be homogeneously immobilized in polymer FPs because of the very short mixing time to form aggregation between NPs. Indeed, we successfully fabricated PI FPs by homogeneously dispersing 12.5 wt% of Au NPs (average size: 5.6 nm) by the emulsion re-precipitation method using a multistep microfluidic system.[20]

In this study, we demonstrated the fabrication of PI FPs encapsulating a large number of TiO_2 NPs (PI FPs/TiO_2 NPs) by the emulsion re-precipitation method as a model compound used for sunscreen and investigated their protection property against UV light.

2. Experimental section

2.1 Materials

Poly(amic acid) (PAA) solution was purchased from Sigma-Aldrich Co. LLC. TiO_2 NP dispersion liquid (rutile type crystals) was developed and supplied by Ishihara Sangyo Kaisya Ltd. *N*,*N*-Dimethylacetamide (DMAc), pyridine, acetic anhydride, and *n*-hexane were purchased from Wako Pure Chemical Industries, Ltd. and were used without any purification.

2.2 Characterization techniques

X-ray diffraction (XRD) pattern of the fabricated PI FPs/TiO_2 NPs was measured by a powder XRD system, SmartLab (Rigaku Corp.). Transmission electron microscopy (TEM) images were collected using FEI Tecnai G2 20. Dynamic light scattering (DLS) analysis was performed with DLS-7000 (Otsuka Electronics Co. Ltd.). Line scan elemental analysis was conducted using a scanning electron microscope (SEM, Hitachi S-4800) attached with an energy dispersive X-ray spectroscope (EDX, Bruker X Flash 6|100). For thermogravimetric analysis-differential thermal analysis (TG-DTA) of the as-fabricated material using TG-DTA2000 (Bruker Corporation) was used. UV-vis transmission spectra of *ca.* 50 μm thick application films, prepared from TiO_2 NPs powder (1.4 wt%) or PI FPs/TiO_2 NPs powder (7 wt% including 1.4 w% TiO_2 NPs)-dispersed in oils used in cosmetics with a mechanical mixer, were collected using a UV-vis spectrophotometer (JASCO V-660).

2.3 Method

Fig. 1 shows a schematic diagram of the fabrication process of PI FPs/TiO_2 NPs under rapid mixing, streaming and heating conditions using micro-mixers, microtubes, and a micro heat exchanger. First, PAA FPs encapsulating TiO_2 NPs (PAA FPs/TiO_2 NPs) were fabricated by the emulsion re-precipitation method as reported earlier.[20,21] Subsequently, PAA FPs were converted to PI FPs by a cyclodehydration reaction, *i.e.*, chemical imidization (Scheme 1). In a typical experimental setup, Y-type micro-mixers (Teflon; YMC Co. Ltd., Japan, channel width = 500 μm) and

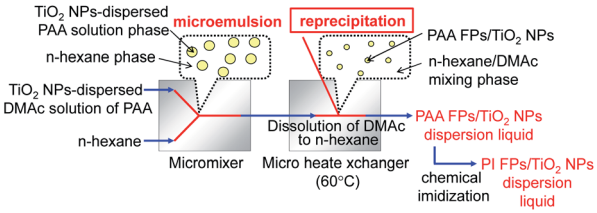

Fig. 1 Schematic diagram of the fabrication process for PI FPs/TiO_2 NPs using a multistep microfluidic system.

a micro heat exchanger (Teflon tube; i.d. = 1000 μm, length = 3 m) connected serially by Teflon tubes (i.d. = 1000 μm, length = 0.15 m) were used. The TiO_2 NPs-dispersed poly(amic acid) (PAA, Scheme 1)/DMAc solution, which was used as a starting material, was prepared by mixing the PAA solution, TiO_2 dispersion liquid, and DMAc because the dispersion stability of TiO_2 NPs was quite good in PAA solution without any dispersion stabilizer. DMAc solution containing PAA (1 wt%) and TiO_2 NPs (0.25 wt%) was introduced into the micromixer through a pump (JASCO PU-2086). The stream of DMAc solution (8.0 mL min^{-1}) was struck against the *n*-hexane stream (20 mL min^{-1}) in the micromixer at ambient temperature, followed by the introduction to a micro heat exchanger at 60 °C through a Teflon tube within 63 ms. In the first step, DMAc droplets in *n*-hexane (emulsion) were formed around the micromixer due to the immiscibility of DMAc and *n*-hexane under the applied condition. In the next step, the emulsion was rapidly heated to 60 °C for few seconds while passing through the heat exchanger. As a result, PAA FPs/TiO_2 NPs were re-precipitated through the dissolution of DMAc into *n*-hexane. The resultant liquid containing PAA FPs/TiO_2 NPs in *n*-hexane/DMAc mixture was collected in a 1 L glass vessel and heated at 60 °C followed by the addition of 5 mL of pyridine and acetic anhydride mixture (1 : 1 mol mol^{-1}) with stirring. After stirring for 1 h, the yellow dispersion liquid of PI FPs/TiO_2 NPs was obtained. This yellow dispersion liquid was then cooled at room temperature under a static condition. In this stage, complete phase separation between *n*-hexane and DMAc including the suspension of PI

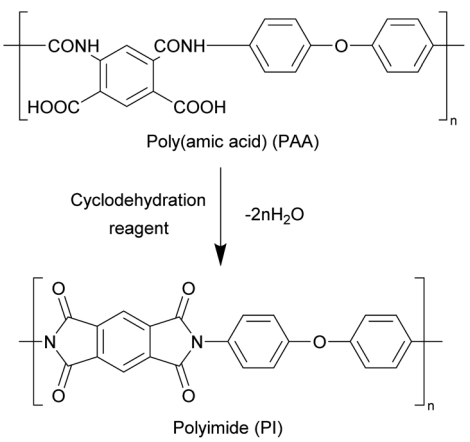

Scheme 1 Reaction scheme to obtain PI from PAA by dehydration.

FPs/TiO_2 NPs occurred. Finally, the *n*-hexane phase was removed, and PI FPs/TiO_2 NPs were separated simply by filtration of the DMAc phase with a membrane filter. The product was washed with methanol and dried at room temperature under reduced pressure.

3. Results and discussion

Fabricated PI FPs/TiO_2 NPs were analysed by several methods (XRD, TEM, SEM, EDX, TG-DTA, and UV-vis spectroscopy). From the XRD pattern of the PI FPs/TiO_2 NPs, the crystal form of TiO_2 NPs is a rutile type structure after fabrication (Fig. 1S†). The average particle size was obtained as 5.6 nm by using Scherrer's equation from the XRD pattern, which is in good agreement with the result of DLS measurement of bare TiO_2 nanoparticles (Fig. 2S†). Fig. 2 shows the TEM images of the as-fabricated PI FPs/TiO_2 NPs at various magnifications. All FPs were spherical, and the average particle size ranges between 150∼200 nm. The particle size distribution profile of PI FPs/TiO_2 NPs measured by DLS is shown in Fig. 3, and the mean particle size is 214 nm, which corresponds well with the TEM observations. There was no drastic change in the size of TiO_2 NPs after fabrication, as observed from the TEM image of bare TiO_2 NPs (Fig. 3S†) with a mean particle size of 5.2 nm. Hence, from the above results, it is suggested that the fabrication process has a negligible effect on TiO_2 NPs. An observation of the TEM images revealed that the edges of all FPs were significantly dark in color, caused by the eccentric location of TiO_2 NPs on the surface of PI FPs. In order to obtain more detailed information on the structure of PI FPs/TiO_2 NPs, line scan elemental analysis with SEM-EDX was executed. The line scan elemental profile monitoring the Ti-Kα (black) and N-Kα (red) lines and a SEM image with the scanned line are shown in Fig. 4a and b, respectively. Intensity of the N-Kα line, derived from PI molecules, was most intense at the center of the FP and decreased as it moved from the center to the edge. We can easily understand that FP is spherical. On the contrary, the intensity of the Ti-Kα line at the center of the FP is the weakest, most intense near the surface of the FP, and rapidly decreased as it progressed towards the outermost surface. These results are attributed to the disproportionately embedded TiO_2 NPs near the surface of the PI FP.[22,23]

Here, we suggest a formation mechanism of the PI FPs/TiO_2 NPs as follows. As shown in Fig. 1, droplets of PAA solution with dispersed TiO_2 NPs are formed in *n*-hexane by the mixing

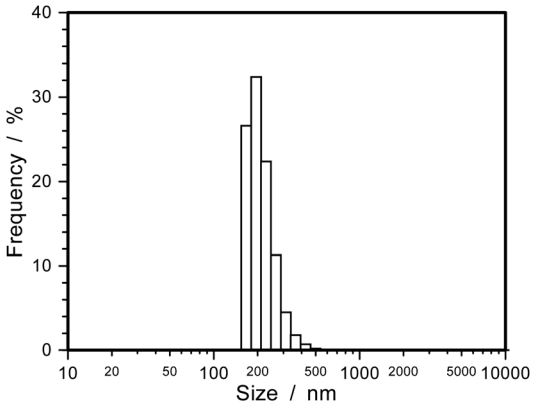

Fig. 3 Size distribution of PI FPs/TiO_2 NPs estimated by DLS analysis.

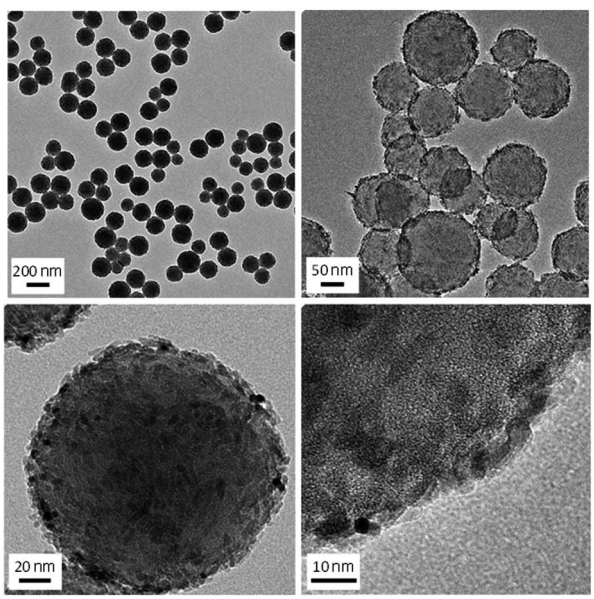

Fig. 2 TEM images of PI FPs/TiO_2 NPs at various magnifications.

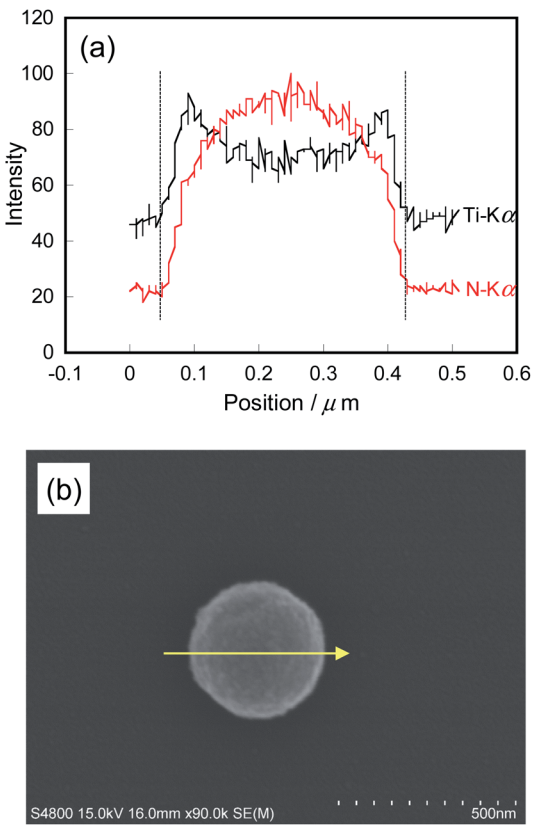

Fig. 4 (a) EDX elemental line scanning profile, (b) SEM image of PI FPs/TiO_2 NPs. Yellow coloured arrow indicates the scanning line.

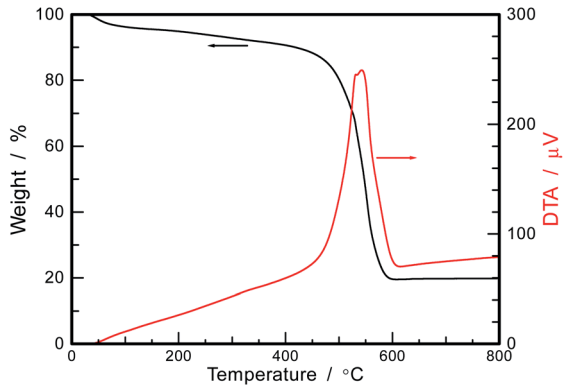

Fig. 5 TG-DTA curve of PI FPs/TiO_2 NPs after drying with particles separated from the dispersion liquid.

process in a micromixer. In the re-precipitation step in Fig. 1, DMAc begins to diffuse into *n*-hexane because the two solvents become miscible due to heating. Consequently, TiO_2 NPs in the droplet of PAA solution move towards the surface accompanied by DMAc and then adsorb at the interface between the droplet (PAA + DMAc) and *n*-hexane. This adsorption phenomenon has been known as Pickering stabilization, by which solid particles can reside at the interface between two immiscible liquids.[24] On the other hand, PAA molecules are still homogeneously dissolved in the droplet. Finally, the structure of FPs is fixed by re-precipitation due to the complete efflux of DMAc into *n*-hexane.

To estimate the mass content of TiO_2 in PI FPs/TiO_2 NPs, TG-DTA was conducted under the airflow condition. As shown in Fig. 5, the weight losses were observed at the temperature regions of ~446 and 446–608 °C. The initial weight loss up to 446 °C is assigned to the removal of solvents at a low temperature (less than about 100 °C), then elimination of water by the thermal imidization, *i.e.*, cyclodehydration, of unreacted PAA above 100 °C. At the second and significant weight loss from 446 to 608 °C, the thermal degradation of PI occurs.[25] Over the temperature of 608 °C, the TG curve gave a constant value of 19.8 wt%, indicating the complete decomposition and removal of PI molecules. Therefore, the TG-DTA results suggested that the content of TiO_2 in PI FPs/TiO_2 NPs was 19.8 wt%, and it agreed with the ratio of TiO_2 to PAA in the starting solution, suggesting that almost all TiO_2 NPs were encapsulated in PI FPs.

We studied the UV-vis transmission property of PI FPs/TiO_2. Fig. 6 shows the UV-vis transmission spectra of application films derived from oils used in cosmetics dispersing bare TiO_2 NPs (1.4 wt%) and fabricated PI FPs/TiO_2 NPs (7 wt% PI FPs/TiO_2 NPs, *i.e.*, 1.4 wt% TiO_2 NPs in the oil), respectively. It should be noted that both dispersion liquids contain the same mass content of TiO_2 NPs (1.4 wt%). For the measurement of PI FPs/TiO_2NPs, an application film derived from PI FPs (not containing TiO_2 NPs) dispersed in oils was used as the reference. As shown in Fig. 6, the film containing PI FPs/TiO_2 NPs gave lower transmittance at the UV-vis region compared to that of the bare TiO_2 NPs. Thus, the film containing PI FPs/TiO_2 NPs can shield UV-vis light with less amount than that of bare TiO_2 NPs. Considering the same amount of TiO_2 in both films and the spectrum not including the absorption of the PI matrix, a secondary structure of TiO_2 NPs, namely agglomerates of bare TiO_2 NPs, probably caused a decrease in the UV-shielding property of films. Superficial TiO_2 NPs of agglomerates contribute to the absorption of UV light, whereas inner TiO_2 NPs were not efficiently used in the absorption of UV light. Indeed, when a dispersion liquid of bare TiO_2 NPs was prepared with a weaker mixing, transmittance of the applied film further increased compared to the film derived from the dispersion prepared with vigorous mixing (Fig. 4S†). This result supports that the agglomerates are resistant towards UV absorption. Thus, PI FPs/TiO_2 NPs revealed superior UV shielding property.

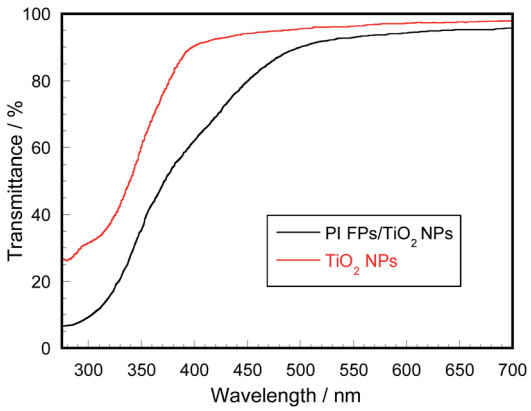

Fig. 6 Transmittance spectra of application films prepared from PI FPs/TiO_2 and bare TiO_2 NPs-dispersed oils.

4. Conclusions

We applied an emulsion re-precipitation technique to achieve fabrication of polymer FP containing NPs using a multistep microfluidic system and have successfully encapsulated TiO_2 NPs up to 19.8 wt% in PI FPs, maintaining the structure and morphology of the NPs. The fabricated material as a model compound for a sunscreen, PI FPs/TiO_2 NPs, was spherical with a diameter of 214 nm and the mean size of TiO_2 NPs was 5.2 nm. Moreover, UV-vis transmission spectra showed high UV shielding efficiency of the PI FPs/TiO_2 NPs as the NPs are located near the surface of the FP. Hence, the developed material could be more effective as a sunscreen material compared to the bare TiO_2 NPs. It is known that PI material has very high biocompatibility and has displayed an insignificant level of cytotoxicity.[26,27] For use as a sunscreen, however, we need to further investigate its stability with respect to acids, alkalis, and UV light and evaluate the Sun Protection Factor (SPF). Based on the results, we must select appropriate polymer matrices.

Conflicts of interest

There are no conflicts to declare.

Notes and references

1 S. Deng, T. Meng, B. Xu, F. Gao, Y. Ding, L. Yu and Y. Fan, *ACS Catal.*, 2016, **6**, 5807–5815.

2 R. Baan, K. Straif, Y. Grosse, B. Secretan, F. El Ghissassi and V. Cogliano, *Lancet Oncol.*, 2006, **7**, 295–296.
3 T. Chen, J. Yan and Y. Li, *J. Food Drug Anal.*, 2014, **22**, 95–104.
4 M. Shakeel, F. Jabeen, S. Shabbir, M. S. Asghar, M. S. Khan and A. S. Chaudhry, *Biol. Trace Elem. Res.*, 2016, **172**, 1–36.
5 J. Wang, J. Wang, Y. Liu, Y. Nie, B. Si, T. Wang, A. Waqas, G. Zhao, M. Wang and A. Xu, *J. Environ. Sci.*, 2019, **85**, 94–106.
6 E. Baranowska-Wojcik, D. Szwajgier, P. Oleszczuk and A. Winiarska-Mieczan, *Biol. Trace Elem. Res.*, 2020, **193**, 118–129.
7 Z. Chen, S. Han, D. Zhou, S. Zhou and G. Jia, *Nanoscale*, 2019, **11**, 22398–22412.
8 A. Weir, P. Westerhoff, L. Fabricius, K. Hristovski and N. von Goetz, *Environ. Sci. Technol.*, 2012, **46**, 2242–2250.
9 Y. Yang, K. Doudrick, X. Bi, K. Hristovski, P. Herckes, P. Westerhoff and R. Kaegi, *Environ. Sci. Technol.*, 2014, **48**, 6391–6400.
10 X. X. Chen, B. Cheng, Y. X. Yang, A. Cao, J. H. Liu, L. J. Du, Y. Liu, Y. Zhao and H. Wang, *Small*, 2013, **9**, 1765–1774.
11 M. Yang, T. Chen, W. S. Lau, Y. Wang, Q. Tang, Y. Yang and H. Chen, *Small*, 2009, **5**, 198–202.
12 F. Caruso, R. A. Caruso and H. Möhwald, *Science*, 1998, **282**, 1111–1114.
13 Y. Kang and T. A. Taton, *Angew. Chem., Int. Ed. Engl.*, 2005, **44**, 409–412.
14 T. K. Bronich, P. A. Keifer, L. S. Shlyakhtenko and A. V. Kabanov, *J. Am. Chem. Soc.*, 2005, **127**, 8236–8237.
15 Y. Kang and T. A. Taton, *Macromolecules*, 2005, **38**, 6115–6121.
16 H. Sertchook and D. Avnir, *Chem. Mater.*, 2003, **15**, 1690–1694.
17 S.-W. Zhang, S.-X. Zhou, Y.-M. Weng and L.-M. Wu, *Laugmuir*, 2005, **21**, 2124–2128.
18 B. Erdem, E. D. Sudol, V. L. Dimonie and M. S. El-Aasser, *J. Polym. Sci., Part A: Polym. Chem.*, 2000, **38**, 4441–4450.
19 I. Csetneki, M. K. Faix, A. Szilágyi, A. L. Kovács, Z. Németh and M. Zrinyi, *J. Polym. Sci., Part A: Polym. Chem.*, 2004, **42**, 4802–4808.
20 T. Ishizaka, A. Ishigaki, M. Chatterjee, A. Suzuki, T. M. Suzuki and H. Kawanami, *Chem. Lett.*, 2012, **41**, 447–449.
21 T. Ishizaka, A. Ishigaki, M. Chatterjee, A. Suzuki, T. M. Suzuki and H. Kawanami, *Chem. Commun.*, 2010, **46**, 7214–7216.
22 M. Li, X. Li, X. Qi, F. Luo and G. He, *Langmuir*, 2015, **31**, 5190–5197.
23 T. Bian, H. Zhang, Y. Jiang, C. Jin, J. Wu, H. Yang and D. Yang, *Nano Lett.*, 2015, **15**, 7808–7815.
24 S. U. Pickering, *J. Chem. Soc., Trans.*, 1903, **91**, 2001–2021.
25 T. J. Shin, B. Lee, H. S. Youn, K.-B. Lee and M. Ree, *Langmuir*, 2001, **17**, 7842–7850.
26 R. R. Richardson Jr, J. A. Miller and W. M. Reichert, *Biomater.*, 1993, **14**, 627–635.
27 S.-Y. Lee, D.-S. Kim, E.-S. Kim and D.-W. Lee, *Sens. Actuators, B*, 2019, **301**, 126995.